Assembly *in vitro* of *Rhodococcus jostii* RHA1 Encapsulin and Peroxidase DypB to form a Nano-Compartment

Rahman Rahmanpour and Timothy D.H. Bugg*

Department of Chemistry, University of Warwick, Coventry CV4 7AL, U.K.

Address for correspondence: Prof. T.D.H. Bugg, Department of Chemistry, University of Warwick, Coventry CV4 7AL, U.K.

Tel 44-2476-573018 Email T.D.Bugg@warwick.ac.uk

Running title: Encapsulin DypB nanocompartment

Keywords: encapsulin; peroxidase DypB, nanocompartment, lignin

Abstract: *Rhodococcus jostii* RHA1 peroxidase DypB has been recently identified as a bacterial lignin peroxidase. The *dypB* gene is co-transcribed with a gene encoding an encapsulin protein, shown in *Thermotoga maritima* to assemble to form a 60-subunit nano-compartment, and DypB contains a C-terminal sequence motif thought to target the protein to the encapsulin nanocompartment. *R. jostii* RHA1 encapsulin protein has been overexpressed in *R. jostii* RHA1, and purified as a high molecular weight assembly (Mr $>10^6$). The purified nanocompartment can be denatured to form a low molecular weight species by treatment at pH 3.0, and can be re-assembled to form the nanocompartment at pH 7.0. Recombinant DypB can be assembled *in vitro* with monomeric encapsulin to form an assembly of similar size and shape to the encapsulin-only nanocompartment, assessed by dynamic light scattering. The assembled complex shows enhanced lignin degradation activity per mg DypB present, compared with native DypB, using a nitrated lignin UV-vis assay method. The measured stoichiometry of 8.6 μmoles encapsulin/μmol DypB in the complex is comparable to the value of 10 predicted from the crystal structure.

Introduction

Several types of bacterial protein-based organelles, or microcompartments, have been characterised in recent years, which consist of polyhedron-shaped arrays of protein subunits, containing enzymes in their interior, that typically catalyse a particular biochemical pathway [1]. Cyanobacteria and chemoautotrophic bacteria contain the carboxysome, an icosahedral complex 80-150 nm in diameter which contains enzymes for CO_2 fixation [2]; the polyhedral Pdu microcompartment in *Salmonella enterica* contains enzymes for 1,2-propanediol utilisation [3]; and the Eut microcompartment in enteric bacteria *Escherichia coli* and *S. enterica* contains enzymes for ethanolamine utilisation [4]. A smaller 240Å icosahedral nanocompartment has been characterised in *Thermotoga maritima*, whose shell-forming protein is called an encapsulin [5]. Homologues of the encapsulin protein are found in *Brevibacterium linens*, where they show antibacterial activity as an extracellular 29 kDa linocin [6], and in *Mycobacterium tuberculosis* [7]. The crystal structure of the *T. maritima* nanocompartment has been determined, containing 60 subunits of encapsulin, enclosing a large central cavity [5]. Sutter et al. have identified a C-terminal peptide extension that appears to target two types of protein to the nanocompartment in different bacteria: a DyP type peroxidase, and a ferritin-like protein [5].

We have recently reported that DypB from *Rhodococcus jostii* RHA1 shows activity as a lignin peroxidase, oxidising a β-aryl ether lignin model compound, or Mn^{2+} ions, or polymeric Kraft lignin [8]. Deletion of the *dypB* gene abolishes the lignin degradation activity of *R. jostii* RHA1 [8], using a colorimetric assay involving nitrated milled wood lignin [9], therefore DypB appears to be important for the lignin degradation activity of this microbe. The genome sequence of *R. jostii* RHA1, a powerful PCB-degrading organism, has been determined [10]. Immediately downstream of the *R. jostii dypB* gene (ro2407) is a 807 bp

encapsulin gene (ro2408), as shown in Figure 1. We therefore wished to investigate whether DypB is packaged within the encapsulin nanocompartment, and examine what effect the nanocompartment has on lignin degradation activity. Here we report the reconstitution of purified recombinant *R. jostii* encapsulin with *R. jostii* DypB to form a packaged nanocompartment.

Figure 1 Genomic context of *R. jostii dypB* gene

Results

Sequence Analysis

In their study of the *Thermotoga maritima* encapsulin, Sutter et al. have identified a 10 amino acid peptide sequence (GSLxIGSLKG) found at the C-terminus of the associated dyp-type peroxidase or ferritin protein, that appears to be responsible for targeting of the protein to the nanocompartment [5]. As shown in Table 1, this C-terminal peptide sequence is present in *R. jostii* RHA1 DypB. A number of bacterial DypB homologues were examined, and their C-terminal amino acid sequences are shown in Table 1. DypB sequences from *Rhodococcus jostii, R. opacus, R. erythropolis, Nocardia cyriacigeorgica, Burkholderia phymatum, B. multivorans, Mycobacterium tuberculosis, Acetobacter pasteuranius, Streptomyces hygroscopicus* and *S. griseus* each show a 20-30 amino acid extension containing the 10 amino acid sequence motif, and in each of these organisms, the *dypB* and encapsulin genes are found immediately adjacent in the respective genomes sequences (see Figure 2). However, DypB homologues from *Pseudomonas fluorescens, Streptomyces coelicolor and S. lividans* lack the C-terminal peptide sequence, and in these organisms, there is no adjacent encapsulin gene. Although the targeting sequence is not always present, there is a clear correlation

between the presence of the C-terminal amino acid sequence motif and the presence of a downstream encapsulin gene.

Table 1. Alignment of C-terminal sequence of bacterial DypB homologues

Expression and purification of R. jostii RHA1 encapsulin nanocompartment

Over-expression of the *R. jostii* RHA1 encapsulin gene in a pET200 expression vector in *E. coli* was found to give rather weak expression of a 29 kDa protein band (data not shown), that upon analytical gel filtration eluted as a low molecular weight protein, suggesting that the assembly to form a nanocompartment had not occurred. Over-expression of the *R. jostii* encapsulin gene in the pTipQC2 expression vector in a *R. jostii RHA1*Δ encapsulin strain, however, was found to give high expression of a 29 kDa protein band by SDS-PAGE (see Figure 2, lane 2). Purification of cell lysate by Superdex 200 gel filtration chromatography gave a major peak at short retention time (see Figure S1, Supporting Information), corresponding to a very high molecular weight protein (predicted 1.8 MDa by calibration with protein standards), consistent with a high molecular weight nanocompartment. Purification to homogeneity was achieved by Mono Q anion exchange, followed by Sephadex 75 gel filtration chromatography (see Figure 2). Elution of the protein complex from Sephadex 75 gel filtration was found to give three peaks, each of which contained the encapsulin monomer by SDS-PAGE, indicating the presence of three different multimeric forms in solution (see Figure S2, Supporting Information).

Figure 2. Purification of *R. jostii* RHA1 encapsulin, monitored by SDS-PAGE.

Disassembly and in vitro re-assembly of the nanocompartment

Using purified *R. jostii* RHA1 encapulin nanocompartment, we have investigated methods to disassemble the nanocompartment, using native SDS-PAGE to monitor changes in native molecular weight. The native nanocompartment appears as a very high molecular weight band by native SDS-PAGE, as shown in Figure 3. Treatment with acetate buffer at pH 3 was found to give a low molecular weight band, eluting at approximately 60 kDa by native PAGE (see Figure 3A), consistent with a dimeric species. When the species obtained by treatment at pH 3.0 was subsequently incubated in 50 mM phosphate buffer pH 7.0 for 30 min, analysis by native PAGE revealed once again the high molecular weight band corresponding to reassembled nanocompartment.

In order to characterise further the dis-assembled and re-assembled protein fractions, they were analysed using dynamic light scattering, which has been used to measure the dynamic radius of protein aggregates in solution [11]. The native purified nanocompartment gave a single peak corresponding to a radius of 22 nm, which matches quite well the 240 Å diameter of the *T. maritima* nanocompartment, determined by X-ray crystallography [5]. A sample of protein treated at pH 3.0 gave a major peak at much smaller size, corresponding to a radius of 1.69 nm. The thickness of the *T. maritima* nanocompartment was found to be 20-25 Å [5], therefore, the observed dynamic radius is consistent with dimeric form of encapsulin. Analysis of the reassembled nanocompartment by dynamic light scattering showed that the reassembled encapsulin nancompartment gave a similar but slightly larger dynamic radius of 31 nm, compared with the native nanocompartment, indicating perhaps a slightly expanded structure.

Figure 3. Disassembly and re-assembly of encapsulin nanocompartment

In order to investigate reassembly with DypB, the "denatured" encapsulin was then mixed with purified *R. jostii* RHA1 DypB [8]. In this experiment, 0.6 mg/ml of encapsulin and 0.2 mg/ml of DypB were used, to prevent the possibility of aggregation and unwanted interactions between encapsulin monomers and DypB molecules, and also reducing the possibility of macromolecular crowding in the denatured state, and a low concentration of DypB was considered to increase the efficiency of encapsulin reassembly. The mixture incubated at 100 mM phosphate buffer, 100 mM NaCl, pH 7.4 for 30 minutes and then was then passed through a Superdex™ 200 gel filtration column, and two major peaks were observed (see Figure S3, Supporting Information). Analysis of the first, high molecular weight peak by denaturing SDS-PAGE revealed two protein bands, corresponding to encapsulin and DypB, whereas the second, lower molecular weight peak revealed that it consisted only of DypB, as shown in Figure 4. These data show that reassembly of DypB into the encapsulin nanocompartment has been achieved.

Figure 4. SDS-PAGE of re-assembled encapsulin/DypB complex

The ratio of encapsulin to DypB proteins in the reassembled complex was investigated. Reassembled encapsulin/DypB complex was heated to 50 ^{o}C for 5 min and consequently sonicated for 3 minute, and then total protein determined by Bradford assay in triplicate. DypB content was assessed by measurement of heme content at 404 nm, and comparison with a DypB standard curve. The molar ratio of encapsulin to DypB was found to be 8.6 µmoles encapsulin/µmole DypB.

Peroxidase Activity of encapsulin/DypB complex

The peroxidase activity of the re-assembled DypB/encapsulin complex was assessed by kinetic assays. *R. jostii* RHA1 DypB has been shown to be active with dye ABTS, which can be assayed colorimetrically at 420 nm, and with nitrated milled wood lignin, which can be assayed colorimetrically at 430 nm [8]. As shown in Table 2, the activity per mg protein of the re-assembled DypB/encapsulin complex is approximately 10-fold lower activity using ABTS than pure DypB, but when corrected for the proportion of the complex present as DypB (8.6 mol encapsulin complex/mol DypB), the peroxidase activity of the DypB enzyme in the complex with ABTS is 70-75% of that of native DypB. Using the nitrated lignin assay [9], the activity of the re-assembled DypB/encapsulin assembly was similar to that of DypB alone, but when corrected for the proportion of the complex present as DypB, the activity per mg DypB is 8-fold higher than DypB alone, indicating that assembly in the encapsulin somehow enhances the lignin degradation activity of DypB.

Table 2. Peroxidase activity of reassembled DypB/encapsulin complex

Discussion

This work has demonstrated that *R. jostii* DypB can be assembled *in vitro* with *R. jostii* encapsulin, consistent with the co-expression of the two genes, and the presence of the C-terminal targeting sequence in DypB. The work also provides procedures for *in vitro* disassembly of the nanocompartment and re-assembly with "cargo" proteins. The nanocompartment might prove to have useful applications for biotechnology, therefore, these procedures could be used to load proteins into the nano-compartment *in vitro*. The data

obtained by dynamic light scattering (see Figure 3B) shows that reassembled nanocompartment is comparable (though not identical) with original nanocompartment, and the diameter of 22 nm agrees well with the diameter of 240 Å determined from the crystal structure of the *T. maritima* nanocompartment [5]. The stoichiometry of 8.6 mol encapsulin/mol DypB also agrees quite well with the stoichiometry of 10 mol encapsulin/mol DypB predicted from the crystal structure, where one nanocompartment containing 60 subunits of encapsulin was predicted to contain 6 subunits of DypB.

The peroxidase activity of reassembled encapsulin/DypB complex provides some interesting clues to the possible functional role of the encapsulin/DypB complex. Using ABTS as substrate, the peroxidase activity of the complex is similar to that of DypB alone, which is surprising, since the pores in the encapsulin nancompartment structure are <5 Å wide, large enough to allow hydrogen peroxide to enter, but not a large dye molecule such as ABTS. It is conceivable that some subunits of DypB might be attached to the exterior of the nanocompartment, but all the binding sites for the C-terminal targeting peptide are located on the inside of the nano-compartment [5]. The other possibility is that the nano-compartment is a flexible, dynamic structure that is able to open and shut to take up substrate molecules. This explanation seems consistent with the observation of other assemblies by gel filtration chromatography (Figure S2, Supporting Information).

The observation that the reassembled encapsulin/DypB complex shows 8-fold higher activity in the nitrated lignin assay (per mg DypB) than DypB alone implies that the encapsulin nano-compartment somehow increases the activity with polymeric lignin. One possible explanation is that it may assist in localising DypB onto the hydrophobic surface of lignin. The non-specific binding of cellulase enzymes to the hydrophobic surface of lignin is thought to slow down the rate of lignocellulose breakdown by cellulases [12], which can be alleviated by addition of non-ionic detergents that preferentially bind to lignin [13].

Furthermore, lignin peroxidase from *Phanerochaete chrysosporium* has been shown to directly adsorb to the surface of synthetic lignin [14], thereby assisting in lignin breakdown. If the encapsulin nano-compartment is a dynamic structure, then it seems possible that it could disassemble on the surface of lignin or lignocellulose, and therefore localise DypB onto the surface of lignin or lignocellulose, as illustrated in Figure 5.

Figure 5. Assembly of nanocompartment and hypothesis for delivery to lignocellulose

One issue that is unresolved is the cellular location of the DypB/encapsulin complex. The lignin degradation activity of *R. jostii* RHA1 was measured using extracellular extract [8,9], implying that DypB is exported from the cell. The encapsulin-related linocins from *B. linens* and *M. tuberculosis* have also been detected extracellularly [6,7], and we have also observed a protein band corresponding to encapsulin in extracellular fractions of *R. jostii* RHA1 (data not shown), and yet the encapsulin nanocompartment has only been observed intracellularly [5]. The mechanism for cell export of encapsulin and DypB is unknown, and would seem not to follow known protein export mechanisms. In summary, the ability to package proteins into the cavity of such a nanocompartment, using a specific targeting sequence, offers interesting possible applications for biotechnology, and may have specific application for biomass deconstruction.

Materials and Methods

Strains. Gene deletion strain *Rhodococcus jostii RHA1* Δencapsulin, in which encapsulin gene ro2408 is deleted, was constructed by Dr. R Singh and Prof. L. Eltis (Dept. Microbiology and Immunology, University of British Columbia), using the method of van der Geize *et al* [15],

as described previously for construction of a ΔdypB strain [8]. The *R. jostii* RHA1 encapsulin gene was expressed on an inducible expression vector pTipQC2 [16] by Dr. Singh, allowing inducible expression of encapsulin in *R. jostii* RHA1.

Expression and purification of R. jostii encapsulin. A 1 litre culture of *R. jostii RHA1* Δencapsulin/pTipQC2 (knockout for genomic encapsulin gene but complemented for encapsulin gene with pTipQC2 plasmid) was grown in the presence of 35 μg/ml chloramphenicol for 36 hours at 30°C, with shaking at 180 rpm. At OD_{600} 0.6, the culture was induced by addition of thiostrepton (final concentration 1 μg/ml), and the culture was grown for a further 16 hr at 30^{o}C overnight, and then cells were harvested by centrifugation at 13,000 *g* (10 min). The cell pellets were resuspended in 10 ml lysis buffer (50 mM NaH_2PO_4, 10 mM imidazole, pH 8.0) in the presence of 1mM PMSF (phenylmethanesulfonyl fluoride), then lysozyme (1 mg/ml) and DNase (2 U per g cell) were added and left at room temperature for 30 minutes. Cell lysis was carried out by sonication (3 x 1 min, 0 ^{o}C). After centrifugation at 13000 *g* (30 min), the clear supernatant was filtered (20 μm) and concentrated to 1 ml using a 50 kDa Amicon centricon device.

The concentrated cell lysate was applied to a Superdex™ 200 gel filtration column, and eluted with 50 mM phosphate buffer 100 mM NaCl pH 7.4 at a flow rate of 0.5 ml/min. Fractions (0.5 ml) showing a 29 kDa band for encapsulin by SDS PAGE were pooled, and exchanged for 20 mM Tris-HCl pH 8.0 buffer using a PD-10 column. The resultant solution was applied to a Mono Q HR 5/5 anion exchange FPLC column, and protein was eluted with a gradient of 0 to 1M NaCl in 20 mM Tris-HCl pH 8.0 buffer. Fractions containing the 29 kDa encapsulin band, which eluted at approximately 700 mM NaCl, were pooled. Further purification was achieved by elution from a Sephadex® *G*-75 column, equilibrated with 50

mM phosphate buffer, 100 mM NaCl pH 7.4 and a flow rate of 0.75 ml/min. Collected fractions containing pure encapsulin (yield 2.5 mg protein) were pooled for further analysis.

Disassembly and reassembly of encapsulin. Purified encapsulin (0.6 mg) was treated in 100 mM acetate buffer pH 3.0 (1 ml) on ice for 15 minutes, and a sample (100 µl) was taken for native PAGE and dynamic light scattering. Then 100 mM phosphate buffer, 100 mM NaCl, pH 7.4 (2 ml) was added to the solution, incubated for 30 minutes on ice. Buffer was exchanged to 50 mM phosphate buffer, 100 mM NaCl, pH 7.4 by two passages through a 10 kDa Centricon device. A sample (100 µl) was taken for native PAGE and dynamic light scattering.

Disassembly/reassembly in presence of DypB. Purified encapsulin (0.6 mg) was treated with 100 mM acetate buffer pH 3.0 (1 ml) on ice for 15 minutes in the presence of DypB (0.2 mg). DypB was shown to be highly active at pH 3, and does not lose activity for this period of time at this pH. Reassembly was carried out as described above, then the solution was injected onto a Superdex™ 200 column equilibrated with 50 mM phosphate buffer, 100 mM NaCl, pH 7.4, and eluted with this buffer with a flow rate of 0.5 ml/min. Samples from each fraction were analysed by SDS PAGE.

Analysis by dynamic light scattering. Analysis of dynamic radius was carried out by dynamic light scattering using a Malvern Zetasizer instrument with laser wavelength of 633 nm, using a 0.1 mg/ml concentration solution (45 µl) in 50 mM phosphate buffer, 100 mM NaCl, pH 7.4 buffer except for disassembled protein which was in 100 mM acetate buffer pH 3.0. Three

measurements were performed at 20°C, each cycle lasting 60 seconds. Data was analysed and presented by Zetasizer Nanoseries software, and the average size for each measurement calculated and recorded.

Assays for peroxidase activity. The re-assembled encapsulin/DypB complex, purified by gel filtration as described above, was assayed using ABTS (2,2'-azino-bis(3-ethylbenzothiazoline-6-sulphonic acid) [8] and nitrated lignin assay [9] procedures. Assays were carried out at 0.2 mg/ml total protein concentration, and compared with pure *R. jostii* RHA1 DyPB, and a buffer-only control. ABTS assay: to enzyme (0.2 mg) in 100 mM acetate buffer pH 5 was added ABTS (10 mM final concentration), 1 mM H_2O_2, in a final volume of 1 ml. Reactions were initiated with the addition of H_2O_2, and initial rates were monitored at 420 nm. Nitrated lignin assay: assays were carried out using a stock solution of nitrated milled wood lignin (0.015 mM, 800 µl), prepared as previously described [9] in 750 mM Tris buffer pH 7.4 containing 50 mM NaCl, to which was added 0.2 mg enzyme and 40 mM H_2O_2 (50 µl), total volume 1.0 ml. Reactions were initiated with the addition of H_2O_2, and initial rates were monitored at 430 nm over 20 min. Control assays were carried out in which protein solution was replaced with 750 mM Tris pH 7.4, 50 mM NaCl.

Acknowledgements

We thank Dr. Rahul Singh and Prof. Lindsay Eltis (Dept. Microbiology and Immunology, University of British Columbia) for providing us with gene deletion strain *R. jostii* RHA1 Δencapsulin and plasmid pTipQC2 containing the recombinant encapsulin gene. We thank the University of Warwick for provision of a Studentship (R.R.), Prof. Alison Rodger (Univ.

Warwick) for advice on dynamic light scattering, and Darren Braddick for practical assistance.

References

1. Yeates TO, Crowley CS & Tanaka S (2010) Bacterial microcompartment organelles: protein shell structure and evolution. *Annu. Rev. Biophysics* **39**, 185-205.

2. Tanaka S, Kerfeld CA, Sawaya MR, Cai F, Heinhorst S, Cannon GC & Yeates TO (2008) Atomic-level models of the bacterial carboxysome shell. *Science* **319**, 1083-1086.

3. Havemann GD, Sampson EM & Bobik TA (2002) PduA is a shell protein of polyhedral organelles involved in coenzyme B_{12}-dependent degradation of 1,2-propanediol in *Salmonella enterica* serovar Typhimurium LT2. *J. Bacteriol*. **184**, 1253-1261.

4. Tanaka S, Sawaya MR & Yeates TO (2010) Structure and mechanisms of a protein-based organelle in *Escherichia coli*. *Science* **327**, 81-84.

5. Sutter M, Boehringer D, Gutmann S, Günther S, Prangishvili D, Loessner MJ, Stetter KO, Weber-Ban E & Ban N (2008) Structural basis of enzyme encapsulation into a bacterial nanocompartment. *Nat. Struct. Mol. Biol*. **15**, 939-947.

6. Valdes-Stauber N & Scherer S (1994) Isolation and characterization of linocin M18, a bacteriocin produced by *Brevibacterium linens*. *Appl. Environ. Microbiol*. **60**, 3809-3814.

7. Rosenkrands L, Rasmussen PB, Carnio M, Jacobsen S, Theisen M & Andersen P (1998) Identification and characterization of a 29-kDa protein from Mycobacterium tuberculosis culture filtrate recognized by mouse memory effector cells. *Infect. Immun*. **66**, 2728-2735

8. Ahmad M, Roberts JN, Hardiman EM, Singh R, Eltis LD & Bugg TDH (2011) Identification of DypB from *Rhodococcus jostii* RHA1 as a lignin peroxidase. *Biochemistry* **50**, 5096-5107.

9. Ahmad M, Taylor CR, Pink D, Burton K, Eastwood D, Bending GD & Bugg TDH (2010) Development of novel assays for lignin degradation: comparative analysis of bacterial and fungal lignin degraders. *Molecular Biosystems* **6**, 815-821.

10. McLeod MP, Warren RL, Hsiao WWL, Araki N, Myhre M, Femandes C, Miyazawa D, Wong W, Lillquist AL, Wang D, Dosanjh M, Hara H, Petrescu A. Morin RD, Yang G, Stott JM, Schein JE, Shin H, Smailus D, Siddiqui AS, Marra MA, Jones SJM, Holt R, Brinkman FSL, Miyauchi K, Fukuda M, Davies JE, Mohn WW & Eltis LD (2006) The complete genome of *Rhodococcus* sp. RHA1 provides insights into a catabolic powerhouse. *Proc. Natl. Acad. Sci. USA* **103**, 15582-15587.

11. Moradian-Oldak J, Paine ML, Lei YP, Fincham AG & Snead ML (2000) Self-assembly properties of recombinant engineered amelogenin proteins analysed by dynamic light scattering and atomic force microscopy. *J. Struct. Biol*. **131**, 27-37.

12. Palonen H, Tjerneld F, Zacchi G & Tenkanen M (2004) Adsorption of *Trichoderma reesei* CBH1 and EGII and their catalytic domains on steam-pretreated softwood and isolated lignin. *J. Biotechnol*. **107**, 65-72.

13. Eriksson T, Börjesson J & Tjerneld F (2002) Mechanism of surfactant effect in enzymatic hydrolysis of lignocellulose. *Enz. Microb. Technol*. **31**, 353-364.

14. Johjima T, Itoh N, Kabuto M, Tokimura F, Nakagawa T, Wariishi H & Tanaka H (1999) Direct interaction of lignin and lignin peroxidase from *Phanerochaete chrysosporium*. *Proc. Natl. Acad. Sci. USA* **96**, 1989-1994.

15. van der Geize R, Hessels GI, van Gerwen R, van der Meijden P & Dijkhuizen L (2001) Unmarked gene deletion mutagenesis of *kstD*, encoding 3-ketosteroid Δ^1-dehydrogenase, in *Rhodococcus erythropolis* SQ1 using *sacB* as counter-selectable marker. *FEMS Microbiol. Lett*. **205**. 197-202.

16. Nakashima N & Tamura T (2004) Isolation and characterization of a rolling-circle-type plasmid from *Rhodococcus erythropolis* and application of the plasmid to multiple-recombinant-protein expression. *Appl. Environ. Microbiol*. **70**, 5557-5568.

Table 1. Alignment of C-terminal amino acid sequence of bacterial DypB homologues. Sequences listed in order of sequence similarity to *R. jostii* RHA1 DypB sequence. [a]Gene annotated as bacteriocin or linocin.

Bacterial strain	Accession number of DypB homologue	C-terminal protein sequence (encapsulin targeting sequence underlined)	Size (aa)	Downstream encapsulin family[a] gene? (accession number)
Rhodococcus jostii RHA1	Q0SE24	ESLGDEPAGAES------APEDPVEPAAAGPYDLSLKIGGLKGVSQ	350	Yes (Q0SE23)
Rhodococcus opacus B4	C1B1V7	ESLGDAPAAAEP------APEDP-APAGASPYELSLKIGGLKGVSQ	349	Yes (C1B1V8)
Rhodococcus erythropolis	C0ZVK5	DDPPDAPTR---------LVPEATFTAPIS---DGSLGIGSLKRSAQQ	341	Yes (C0ZVK4)
Burkholderia phymatum	B2JNZ7	EALADREPQPASAS----AAASADTFACAEPGHDGSLNIGSLKGTAQYE	352	Yes (B2JNZ6)
Burkholderia multivorans	A9ATN5	DALPDRAAPAEAAA----PAPSSN-----EPHRDGSLKIGSLKGVKSV	353	Yes (A9ATN4)
Mycobacterium tuberculosis	O07180	DHPP-------------PLPQAATPTLAA----GSLSIGSLKGSPR	335	Yes (O07181)
Nocardia cyriacigeorgica	H6R1G4	DDLPDPPG----------ASPADDATPAAPAADGSLGIGTLKRSS	341	Yes (H6R1G5)
Streptomyces coelicolor	Q9FBY9	EDLPARP	316	No
Streptomyces lividans	D6EC39	EDLSARP	329	No
Streptomyces hygroscopicus	H2JMY8	EDLPEPPAAG-------AVAAVTPTDSQVRSSGSSLGIGSMKRSMSR	349	Yes (H2JMY9)
Streptomyces griseus	B1VSP6	DAPPPPPAPARTGNLPEPVPAPVRQEPPAAGADHGSLRIGSLQESAQ	357	Yes (B1VSP6)
Acetobacter pasteurianus	C7JE82	DDAPNMSTENTQ-----ASPEPVTAPPLPKALHGSLGIGSLNNKDA	379	Yes (C7JE83)
Pseudomonas fluorescens	Q4KA97	EDLAERAPTGL	328	No
Pseudomonas fluorescens	I2BZP5	EALPDREPVA	320	No
		Sequence motif GSLxIGSLKG		

Table 2. Peroxidase activity of reassembled DypB/encapsulin complex. Assays were carried out using 0.2 mg protein (either purified DypB or reassembled encapsulin/DypB complex) as described in Materials and Methods.

		DypB only		DypB/encapsulin assembly	
Substrate	Control (ΔA/min)	Rate (ΔA/min)	Activity per mg protein	Rate (ΔA/min)	Activity per mg DypB
ABTS	0.00023 ± 0.0001	0.81 ± 0.01	4.05 ± 0.05	0.055 ± 0.01	2.75 ± 0.5
Nitrated lignin	0.0025 ± 0.0004	0.0074 ± 0.001	0.025 ± 0.005	0.0071 ± 0.0016	0.20 ± 0.08

Figure Legends

Figure 1. Genomic context of *Rhodococcus jostii* RHA1 *dypB* and encapsulin genes.

Figure 2. Purification of *R. jostii* RHA1 encapsulin. Figure shows SDS-PAGE analysis of pooled fractions from cell extract, Superdex 200 gel filtration chromatography, MonoQ anion exchange, and Sephadex 75 gel filtration.

Figure 3. Disassembly and reassembly of encapsulin nanocompartment. A. Native SDS-PAGE analysis of: native encapsulin nanocompartment; treatment at pH 3.0 leading to disassembly; reassembly at pH 7.0. B. Analysis of the same samples by dynamic light scattering, showing the predicted particle diameter.

Figure 4. Purification of reassembled encapsulin/DypB complex by Superdex 200 gel filtration. Analysis by SDS-PAGE shows the presence of encapsulin and DypB in the high molecular weight complex (1^{st} peak), and only DypB in the 2^{nd} lower molecular weight fraction.

Figure 5. Assembly of nanocompartment and hypothesis for delivery to surface of lignocellulose.

Figure 1

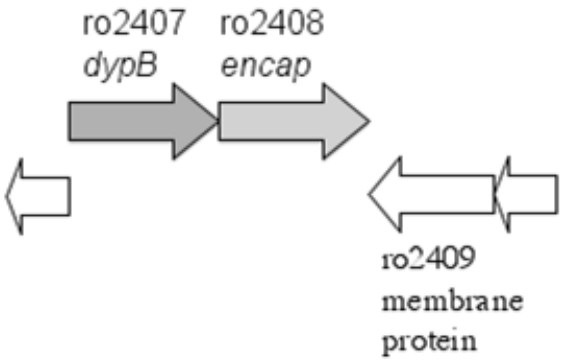

Figure 2

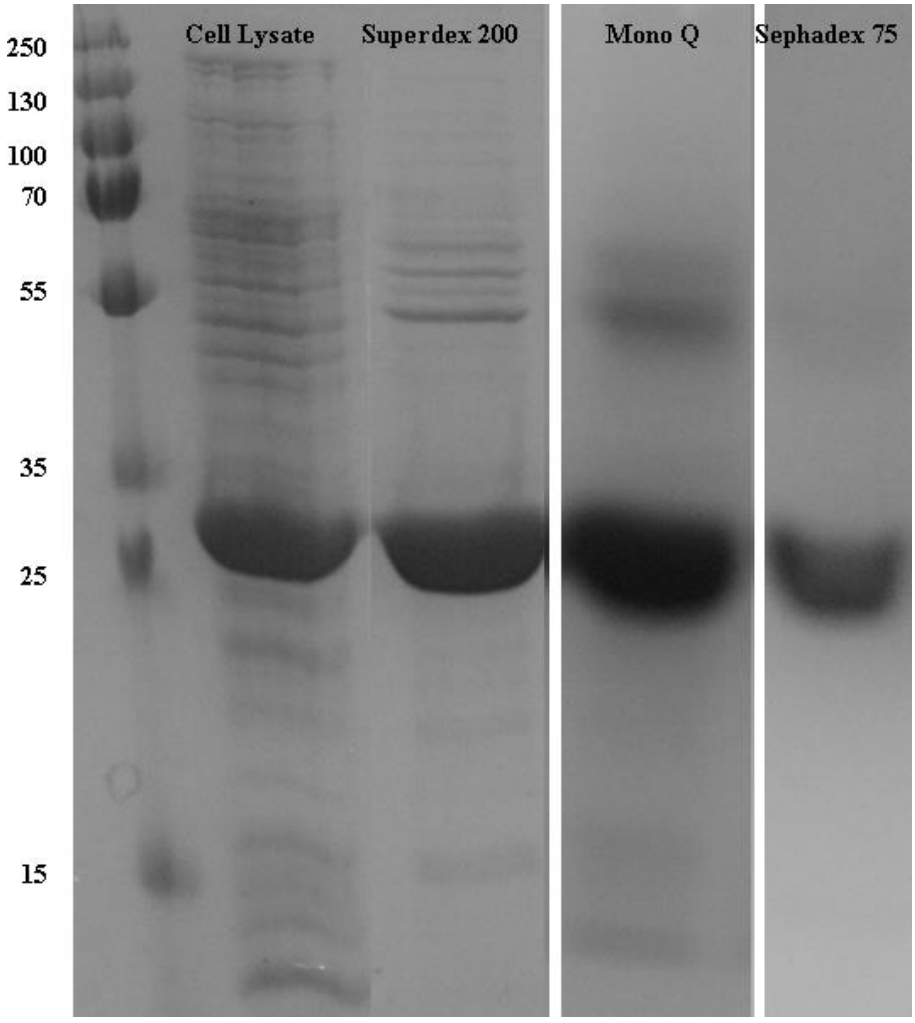

Figure 3

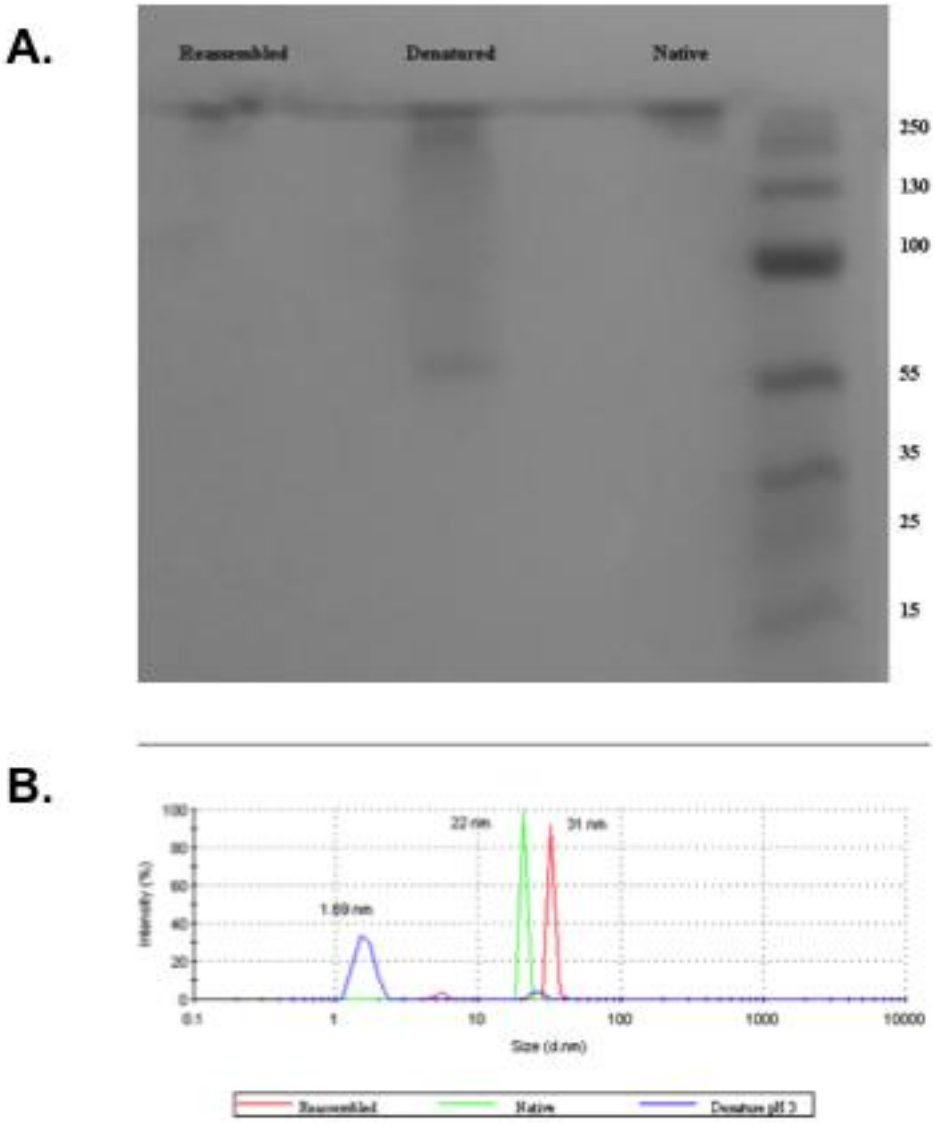

Figure 3

Figure 4

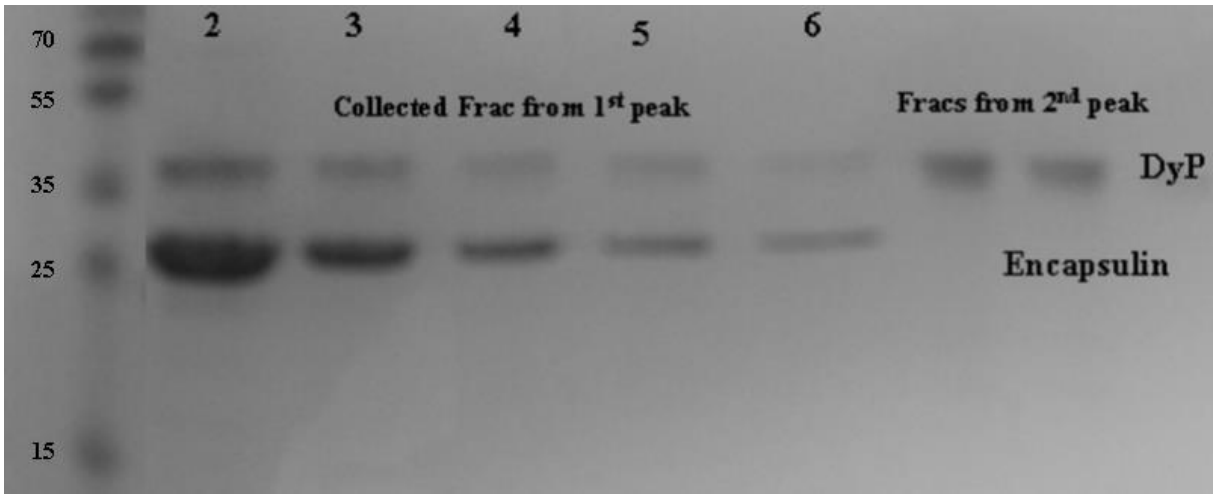

Figure 5